Penetration of Carbon-Fabric-Reinforced Composites by Edge Cracks During Thermal Aging

Kenneth J. Bowles and John E. Kamvouris
Lewis Research Center
Cleveland, Ohio

July 1994

Penetration of Carbon-Fabric-Reinforced Composites by Edge Cracks During Thermal Aging

Kenneth J. Bowles and John E. Kamvouris

National Aeronautics and Space Administration

Lewis Research Center

Cleveland, Ohio 44135

INTRODUCTION

Thermo-oxidative stability (TOS) test results are significantly influenced by the formation and growth or presence of interlaminar and intralaminar cracks in the cut edges of all carbon-fiber-crosslinked, high-temperature polymer matrix composites[1-5] (i.e., unidirectional, cross-plied, angle-plied, and fabric composites). The rate of thermo-oxidative degradation of these composites is heavily dependent on the surface area that is exposed to the harmful environment and on the surface-to-volume ratio of the structure under study. Since the growth of cracks and voids on the composite surfaces significantly increases the exposed surface areas, it is imperative that the interaction between the aging process and the formation of new surface area as the aging time progresses be understood.

The development and growth of such cracks and voids can be monitored by standard metallographic practices and by liquid-enhanced x-radiography using a liquid such as di-iodobutane. The information obtained is somewhat qualitative. Other than depths of damage and distance between cracks, these procedures provide no quantitative data that can be used to gain an understanding of the mechanisms that significantly influence the thermo-oxidative degradation of these materials.

Composite test specimens have two general surfaces: molded (S_1), which is normally resin rich, and cut, which contains bare fiber surfaces. The importance of obtaining data on the degradation of these surfaces is important because of the need to reduce fabrication costs of carbon-fiber-reinforced composites. Mass production of many small or medium composite structures can be accelerated by machining parts from stock material rather than by using a molding process; however, any machining step produces structures with damaged, bare fiber sides and ends. These surfaces may be exposed to a hostile environment such as high humidity and temperature. Knowing the effect of these environments on the cut surfaces is necessary to project the lifetime and restrictions for the composite structures.

The purpose of this work was to characterize the thermal degradation of carbon fabric-reinforced PMR-15 polyimide composites by investigating the formation of edge cracks in composites of different geometric designs. To augment the metallographic and radiographic examinations, a simple, innovative water immersion technique was developed to quantify the amount and distribution of the crack volume generated by

the aging process. The crack volume was assumed to indicate the relative magnitude of the crack surface area. The results clarified the relationships between crack formation and growth and the thermal degradation of fabric-reinforced composites.

The immersion procedure used water uptake measurements of the aged specimens at various stages of the aging process. The information was then used to clarify relationships which greatly influence the paths by which weight is lost from the test specimens during TOS tests. Additional information was gained from a simple ethanol permeation test. The information presented herein demonstrates the usefulness of these methods in analyzing the thermo-oxidative degradation process for these materials.

EXPERIMENTAL

Materials

In this study, PMR-15 polyimide composites reinforced with T650-35 24-by-23, 8-harness satin carbon fiber fabric were used with a stacking sequence of 0°/90°. The composites were fabricated by autoclave techniques at 316°C. The molded surfaces exhibited a roughened appearance from the bleeder cloth that was used. The cure was followed by a 16-hour freestanding postcure in an air-circulating oven at the same temperature. All processing was done at the General Electric Aircraft Engine Plant in Evendale, Ohio. The specimen designations, nominal dimensions, and surface areas are presented in Table 1. The dimensions were selected to provide specimens with a variety of molded (resin-rich areas adjacent to the vacuum bag containment materials) and cut surface areas. Cut surfaces varied from 2.7% to 89% of the total specimen surface. The specimen designations in Table 1 reflect the nominal percent edge area. Previous studies[1-5] with unidirectional composites showed that the greatest weight loss rate is located at the cut surfaces containing fiber ends (Figure 1). The material in this study had less than 2% void contents and was free of delaminations. Figure 2 shows a typical photomicrograph of the material (prior to aging) with some resin-rich areas between the tows.

Test Procedures

The composite specimens were aged in air-circulating ovens at 288°C, 316°C, and 343°C with an air flow rate of 100 cm^3/min. The specimens were removed from the ovens at regular intervals and placed in a desiccator where they cooled to room temperature. The specimens remained in the desiccator until they were ready to be weighed.

The immersion testing procedure was simple and required only a few pieces of equipment. The procedure measured the amount of crack volume generated by the thermal aging. The specimen was dried for 24 hours in an air-circulating oven at 125°C until the weight stabilized at a fixed value[6]. The specimen was placed in a desiccator while it cooled to room temperature. The weight was then recorded and the specimen was

2

returned to the oven for approximately 15 minutes to return its temperature to 125°C. The specimen was then removed from the oven and immediately quenched by immersion in a distilled water bath.

The bath was large enough to maintain a constant temperature in the bath during the immersion period without the use of wetting agents. The specimen remained in the bath for 5 minutes and was turned periodically to ensure that all sides contacted the water for equal amounts of time. The immersion time was monitored with a stop watch. After the 5-minute soak period, the specimen was removed from the water, patted dry with paper towels, and placed on an analytical balance. Weight measurements were recorded for 50 minutes. Weight readings were recorded every 30 seconds for the first 5 minutes and then at 1-minute intervals for the next 5 minutes. Two more readings, monitored with a stop watch, were taken at 5-minute intervals, followed by two more at 15-minute time spans. The details of the data acquisition can be altered to fit the circumstances of any particular test.

The composite test pieces were then returned to the 125°C oven to reduce their water content to zero. This process normally takes about 15 to 20 minutes after the 5-minute exposure, although it has taken 24 hours at 125°C to eliminate water from similar composites[6]. In this study, the short time for eliminating water indicated that the composite specimens did not become saturated during the 5 minutes of immersion and that the water pickup was confined to the crack and void surface areas.

In some instances, only selected pairs of surfaces (e.g., molded), were exposed by masking the other faces using silicone rubber sheets backed with fiberglass-reinforced epoxy sheet material. The masking materials were held in place by small C-clamps or spring-loaded forceps to permit the investigation of crack formation and progression into the different specimen surfaces.

RESULTS AND DISCUSSION

Metallographic Examination

Standard metallographic examination of the composite specimens was conducted to identify the type of damage that occurred throughout the specimens as they aged. The specimens were sectioned after aging and were then polished and examined. The photomicrographs of composites shown in Figure 3 reveal the absence of significant damage in the T-3 composite. The specimens were aged for 500 hours at 316°C and had a weight loss of 2%. Some resin-rich areas were evident between tows. In contrast, the T-3 specimen in Figure 4 has slightly more damage from 890 hours of aging at 316°C and a 4.4% weight loss. The damage consisted of interlaminar ply cracking and some attack at the ends of the fiber tows. The exposed ends of the specimen are marked. The polished, cut surface shows no visible void areas. Some cracking has occurred in the interior plies, but not in abundance.

Figure 5 shows a T-5 specimen that was aged concurrently with the T-3 specimen of Figure 4. The depletion of matrix resin in the fiber end tows at the exposed end is identical to that shown in Figure 4 for the T-3 specimen; however, the weight loss for the T-5 specimen was 2.9% rather than the 4.4% exhibited by the T-3 specimen. The difference in the weight loss percentages was attributed to the additional four central plies that did not experience weight loss and were protected from the ambient environment. Gross damage, which occurred during aging for 1510 hours at 316°C with a 10% weight loss, is shown in Figure 6. It cannot be determined from these photographs whether there is any interconnection of the cracks that developed during aging.

X-Radiography Results

Figures 7 to 9 show x-radiographs of some of the thinner specimens that had all surfaces brushed with di-iodobutane and then had the excess liquid wiped off. The di-iodobutane enhances the contrast between the sound material and that which contains cracks and voids. The presence of the liquid is characterized by a darker tone. Figure 7 compares a T-3 specimen (top) that was not treated with di-iodobutane with one that was treated (bottom). The specimen on the top appears to be very transparent.

The T-5 (2.9%) specimen shown in Figure 8 was aged for 840 hours at 316°C. The T-5 specimen was x-radiographed under the same conditions (3 minutes at 36 kV) as the previous specimens. Note that the dark stripe in this specimen's perimeter has a width of about 0.9 mm. Water pickup measurements indicated that the specimen contained 0.785 ml of crack volume. The thickness as shown in Table 1 is approximately 0.28 cm, or about twice the thickness of the T-3 panel, suggesting that for these panels, the molded surfaces and the central volume of the composite may contain a total density of cracks and voids that is less than that of the cut edges.

Figure 9 presents two sets of specimens from the T-5 laminates. The specimens on the top were not aged, but the specimen on the bottom was aged at 316°C for 1730 hours and had a weight loss of 9.6%. The contrast in shading between the two specimens indicates that the as-fabricated laminate contains little or no physical damage. Only two of the edges of the aged composite were brushed with di-iodobutane. Although the damage in the aged specimen was very heavy at the two treated edges, as indicated by the deep black stripes in Figure 9, it maintained an even, dark tone throughout the rest of the plate. The width of the damaged edge, measured with an x-y Nikkon digital indexer, was about 1.5 mm. The width of the deep black stripes varied from 1.12 mm to 1.87 mm. The shading differences indicate that more damage is also distributed throughout the surface area of the specimen and possibly throughout the volume.

Crack Depth Tests

Further work was done to obtain additional data needed to investigate the magnitude, depth of penetration, and primary intrusion sites of the cracks into the test specimens. Specimens from the T-3, T-9,

4

T-73, and T-89 groups were treated with drops of ethanol after being dried at 125°C. The drops were carefully placed on the longer cut surfaces of the T-73 and T-89 specimens to determine whether they would penetrate the widths of the blocks. The ethanol penetrated the cut surfaces of both specimens (Table 2). Continuous cracks developed through the widths of the T-89 specimens from cut face to cut face after a weight loss of about 3% was attained. In contrast, the wider T-73 specimens (0.71 cm) allowed only traces of ethanol to completely penetrate through a highly localized strip along its central volume that was aged at 316°C for 1370 hours. The central volume appeared to be cracked. From the data measured from the x-radiographs, the maximum T-73 specimen width that would allow ethanol penetration, would probably be more than 0.224 to 0.374 cm. This nominally agrees with the information presented in Table 2. The ethanol completely penetrated the T-89 specimen at about 10% weight loss but only penetrated an isolated area in the T-73 specimen.

At weight losses as high as 10%, the molded surfaces of specimens T-3 and T-9 showed no evidence of ethanol penetration through the thickness. These data suggest that most of the crack volume is concentrated in the cut edges and that the continuous path of cracks that traverse the width is not present between the two molded surfaces.

Initial Water Pickup and Retention Results

Plots of the data acquired by the water immersion technique are shown in Figure 10. The data are presented in terms of water absorption (g) as a function of time (minute) after surface wiping. The initial weight measurement after wiping the specimen was designated as the zero time measurement and indicated the total amount of water picked up during the immersion time. The plots show the data for different sized specimens and for different aging times. Although not shown in Figure 10, the water pickup weights that were observed reached values as high as 9.6 g. This significant amount of pickup probably represents a large amount of new area. By dividing it by the water density, the retained water weight can be converted to the volume created during aging. A density value of 1g/ml was used. The calculated water volume is assumed to be equivalent to the crack volume.

Two different water pickup curves are shown in Figure 10. Initially, the curves representing the T-89 specimen data show a decrease in retained water along with a slight decrease in the rate of water loss. The data then appear to follow a constant negative slope. The T-9, T-12, and T-73 (specimens with small edge area amounts) data appear to asymptotically approach a constant value after a noticeable decrease in slope during the initial weighing time of 5 minutes. The slopes vary with specimen dimensions and imply the magnitude of crack size change that occurs at the air-water interface as the water evaporates. The slopes also suggest that the interface recedes into the interior of the specimen.

The reduction in weight loss rate may have been a result of the rapid water evaporation from the surfaces of the specimens with high S_1 to $S_2 + S_3$ areas (Figure 1 and Table 1). The molded surfaces have

fewer cracks and initially, those that do exist do not penetrate as deeply as those in the edges. Another cause of the reduction in the weight loss rate may be the decrease in retained water surface area caused by the decrease in the number of cracks and/or the widths of the cracks as the water surface recedes into the composite. A third possibility is the reduction of the water vapor pressure: as the cracks decreased in width, the air-water interface radius of curvature is reduced. This phenomenon is described by the Kelvin equation[7]. The width of the cracks that were observed by microscopy measured about 0.6 mm, producing a reduction to only 99.9% of the normal vapor pressure. Crack sizes on the angstrom level are necessary to make a significant reduction; therefore, the situation this equation describes is not applicable for analyzing the water immersion technique.

The damage band along the exposed edges in Figures 7 to 9 indicate a finite volume of free space for water to be retained. The decrease in shading (Figures 8 and 9) indicates a sharp reduction from the amount of open volume available at the edges to the amount available in the interior of the composites. It is proposed that the initial decrease in weight is caused by the evaporation of the water from the relatively large surface area along the exposed cut surfaces which show very dark shading in the x-radiographs. When this water evaporates, the smaller area of water surface is then exposed to the environment and the reduction in surface area water causes the evaporation rate to decrease. The cracks or voids that are present away from the edge damage must be microscopically visible since the amount of water retained in them is a large fraction of the amount originally picked up (Figure 10).

The curves that show a constant rate of weight reduction for the T-89 specimens in Figure 10 probably reflect the presence of large cracks of almost uniform dimensions through the specimen width. In contrast, the data from the other specimens asymptotically approach a constant weight value probably because the number and widths of the cracks decrease as the water-air interface recedes into the composite. The data for specimen T-73 appear to show a combination of both types of curves, initially following the slopes of the T-89 specimens and then gradually decreasing but not as much as the T-5 and T-12 specimens. This suggests that the crack widths remain constant through most of the specimen width but start to decrease in size or number near the middle.

Reproducibility

Tests were run using two different specimens to determine the statistical reliability of water immersion testing. A T-9 specimen (high molded area and high crack volume content) and a T-73 specimen (high cut surface and high crack volume) were subjected to ten 125°C bakeout and water immersion cycles. The dry weight and wet weight were measured and appeared to be very reproducible. The water pickup was calculated and the data proved to be normally distributed with no evident time trends. The mean weight value and N-1 (N = the number of data points) standard deviation were calculated for each type of measurement. The

6

t-distribution tables showed a value of 2.262, which was used to calculate the 95% confidence intervals. The statistical values are presented in Table 3.

Initial Water Pickup

The reproducibility of the water pickup data encouraged the further study of the void or crack volumes in the aged composites created during aging. Figure 11 shows data for different sizes of polymer matrix specimens reinforced with carbon fabric. The crack volume data, calculated from the initial water pickup values, are plotted as a function of percent isothermal weight loss for each type of specimen. The data fall on separate curves which appear to be linear over the range of weight losses that were investigated. There appears to be no particular order of curve position in relation to the magnitude of the edge fraction. The crack volumes are calculated from the difference between the specimen weight after conditioning at 125°C and the zero time weight measured after the exterior liquid has been removed by wiping.

Previous work with unidirectional composites has shown that cut edges of TOS test specimens greatly influence the weight loss rates during isothermal aging. The greatest weight losses occur at those surfaces containing cut fiber ends[1-5]. Because of these findings, the crack volume per unit cut edge area was plotted as a function of percent weight loss and the results are presented in Figure 12.

The cut edges of the fabric-reinforced specimens are different from those of the unidirectional model in Figure 1 because they consist of 50% S_2 and 50% S_3 surfaces. The data for the T-3, T-5, and T-12 (Table 1) specimens are represented by a single straight line in Figure 12. These specimens have the same molded areas (lengths and widths) and differ only in the cut edge areas. The data from these three specimens indicate that the cut edges are the principal sites for crack formation. The test data from the specimens with the larger molded areas lie significantly below the curve, indicating that they do not correlate with the test data of the experiments with small molded areas (Figure 12).

Water Pickup Density of Surfaces

A slightly different series of immersion tests were conducted to explore the reasons for differences in the crack volume per unit edge area relationships between the large and the small specimens. Each specimen surface was examined in pairs, including molded surfaces, long cut sides, and short cut sides. Each pair of surfaces was masked by silicone rubber sheets backed with fiberglass-epoxy sheet material before being immersed in the water. The masking was held in place by small C-clamps or spring-loaded forceps. Water retention was measured for each set of surfaces and the respective crack volumes and crack volumes per unit edge area were calculated.

Tables 4 and 5 show the crack volume and crack volume density (g/cm^2) for the three different surfaces of the T-5, T-9, and T-73 specimens. The crack volume densities are greater for the end surfaces than for the

other two surfaces of the T-73 and T-9 specimens. This is not the case for the molded areas of the larger T-5 specimen. This suggests that there is much less interaction between the edge cracks in the larger specimen than there is in the smaller specimens. It is possible that the interaction occurs at the corners within a small finite edge length which becomes more significant as the edges become shorter. The end surface crack density is greater than that of the side surfaces of the small specimens; this difference in density occurs because the volume of cracks that are accessible through the end surfaces is approximately equal to the volume that is accessible through the side surfaces. As measured with no surfaces masked off, the total measured crack volume as calculated from the weight pickup for each specimen is larger than that of either cut surface, but significantly less than the total of the two cut edges. This phenomenon is a result of some of the crack volume being measured twice, suggesting that both surfaces are accessible to the same crack voids within the specimens. However, since the magnitude of the crack volume presented in Table 4 is less than the sum of the number of crack voids accessible to each surface, not all cracks or voids are accessible to both types of surfaces. The total measured volumes of the T-9 specimen edges is close to that of the total measured volume.

Thermo-Oxidative Stability Results

As previously stated, the purpose of this work was to characterize the thermal degradation of carbon-fabric-reinforced PMR-15 composites by investigating the formation of edge cracks in composites of different geometric design. To be determined was whether the data presented in Water Pickup Density of Surfaces could be used to predict the material weight loss as a function of time at a particular temperature. The significance of the data that has been obtained is that the specimen geometry affects the accessibility of internal voids to the exposed specimen surfaces, especially the cut edges.

Figure 13 shows data that compare 316°C weight losses for the different size specimens (Table 1) at different aging times. The weight loss data are presented as weight loss per total surface area. Testing was curtailed when the weight loss of a specimen reached 10% or greater. Except for the T-9 composite, the weight loss curves are positioned in the order of their percent of cut surface area after 700 hours of aging. Prior to that time, the curves are grouped into two sets: edge surfaces comprising 26% or less of the total surface area and edge surfaces of greater than 26% of the total surface. The T-3 and T-9 composites have identical thicknesses and data. These results suggest that the weight losses from the cut edges are significantly greater than those of the molded surfaces and they control the overall weight loss of the specimens.

As mentioned in the Initial Water Pickup section, the exposed cut edges of the fabric-reinforced composite specimens are composed of about 50% fiber ends and 50% fiber sides, indicating that the mechanism involved in the oxidation of the cut edges is identical for all four edge surfaces. When calculating the weight loss per unit surface area for the molded and cut surfaces[1-5] using only two types of surfaces and data from two specimen sizes, the values are consistent with those calculated for the large T-3, T-5, T-12, and T-27 specimens

in other composite TOS studies[1-2]. However, some allowances must be made for initial weight losses because of the inconsistencies in smaller specimen data that are mathematically analyzed.

There is no correlation in weight loss per unit area for the smaller molded area specimens. This is probably a result of the differences in the percent weight loss values inherent in specimens of different dimensions. The dimensions directly affect the surface-to-volume ratio upon which the percent calculation is based, resulting in different values for specimens that have the same aging temperature and time. The weight loss value for a set of time-temperature conditions can only be determined if it is assessed on a weight-per-unit-area basis or the specimen dimensions are presented in order to make a comparison by data normalization.

The water immersion tests indicated that three different internal volumes per unit surface area were available to the three types of specimen surfaces, making the effective surface area for each type of surface unique. Mathematical analysis gives reasonable weight loss values using data from three different sizes of specimen that have one set of molded surfaces and two types of cut surfaces. The molded surfaces display the least amount of weight loss per unit area and the cut surfaces display the greatest amount. These values also reflect the results of the water pickup studies presented in Tables 4 and 5. Weight loss data from TOS studies conducted on T-9, T-50, T-73, and T-89 specimens at 288°C, 316°C, and 343°C respectively are shown in Figures 14 to 16. The molded surfaces exhibit the lowest weight loss per unit area for the time span that was studied at all three temperatures. In contrast, the end surfaces lose weight at the fastest rate.

Also included in Figures 14, 15, and 16 are 288°C, 316°C, and 343°C TOS data, respectively, for the three surfaces of unidirectional T-650-35 fiber-reinforced PMR-15 polyimide composites. These composites were fabricated by a simulated autoclave technique to produce the same molded surface texture as the fabric composites. It is evident that the weight loss characteristics of the two types of specimens are similar, except for the differences in the weight loss rates from the S_3 surfaces. The weight loss from the molded and the long cut surfaces of both composites are similar with the exception of the 343°C data. The weight loss data for the unidirectional S_2 surface becomes greater than those for the molded and S_3 surface in Figure 16, although no reason for this behavior is evident at this time. In contrast, the corresponding end surfaces lose weight at different rates with the unidirectional specimens accelerated significantly more than the fabric-reinforced specimens. These differences are probably caused by the unrestricted lengthwise growth of end cracks through the thickness toward the center of the unidirectional specimens. Since the fibers are not bound in place as are the woven fabric fibers, accelerated growth occurs. Complete extension of cracks across the thickness of the fabric composites is restricted by the woven fibers. From these data, it appears that TOS testing of unidirectional composites produces data that are conservative with respect to the behavior of fabric test specimens. The fabric-reinforced composites oxidize at a rate either equivalent to or less than the unidirectional composites depending on the geometry of the test specimens.

CONCLUDING REMARKS

The following conclusions have been derived from this study:

1. The water retention technique is a valuable research tool that can be used to compare crack growth behavior along the cut edges of different size carbon-fabric-reinforced composites.

2. The growth of cracks in the edges of carbon-fabric-reinforced composite cut edges can help to identify the mechanisms involved in the thermal aging of these materials.

3. Unidirectional carbon-fiber-reinforced composite thermo-oxidative stability data can be used as a conservative predictor of carbon fabric composite behavior during elevated temperature aging.

4. The analysis of the results and the developed mechanism(s) can be used to model the isothermal behavior of these materials for dimensions within the range that were investigated in this study.

SUMMARY OF RESULTS

The results conducted on PMR-15 composites herein are as follows:

1. During aging at elevated temperatures, the damage incurred begins at the surface.

2. Cracks that form produce an interconnected network of cracks that progressively increase the surface area of the composite specimen exposed to the ambient atmosphere.

3. The pathways of cracks exist in a more continuous manner through cut edges than they do from one molded surface to the other.

4. The measurement of water pickup is reproducible.

5. Nearly half of the absorbed water is contained in a small width of volume along the cut edges of the aged specimens.

6. There is an interaction of the damage that is formed on all surfaces, which appears to become more significant as the molded surfaces decrease in size and the quadrilateral shape becomes more unsymmetrical.

7. The crack density (cracks per unit surface area) appears to be the greatest for the shorter cut edge and the least for the molded surface.

8. The weight losses of carbon-fabric-reinforced composites relies on the material losses from the cut edges.

9. The weight losses from the cut edges are affected by the new surface areas that are created because of the formation and growth of cracks into the body of the composite specimen and exposure to the oxidizing atmosphere.

10. Differences in the rates of weight loss from the various surfaces reflect their crack volume densities.

11. The water pickup and retention procedure is valuable in determining the significant events involved in the thermal oxidation of carbon-fiber-reinforced polymer matrix composites. This procedure is potentially

useful for clarifying the role of thermal damage in enhancing the progress of the thermal oxidation in the body of the composite structure and for creating an analytical description model the event for predictive uses.

ACKNOWLEDGEMENTS

REFERENCES

1. K.J. Bowles, and A. Meyers, "Specimen Geometry Effects on Graphite/PMR-15 Composites During Thermo-Oxidative Aging," Proceedings of 31st International SAMPE Symposium and Exhibition, J.L. Bauer and R. Dunaetz, eds., Society for the Advances of Materials and Process Engineering, Covina, CA, 1986, pp. 1285-1299.

2. K.J. Bowles, and G. Nowak, "Thermo-Oxidative Stability Studies of Celion 6000/PMR–15 Undirectional Composites, PMR–15, and Celion 6000 Fiber," Journal Composite Materials, 22, (1988), pp. 966–985.

3. K. J. Bowles, "Thermo-Oxidative Stability Studies of PMR–15 Polymer Matrix Composites Reinforced With Various Continuous Fibers," SAMPE Quarterly, 21, (1990), pp. 6–13.

4. F.J. Magendie, "Thermal Stability of Ceramic and Carbon Fiber Reinforced Bismaleimide Matrix Composites" Master's Thesis, Department of Chemical Engineering, University of Washington, Seattle, WA, 1990.

5. J.D. Nam, and J. C. Seferis, SAMPE Quarterly, 24, (1992), pp. 10–18.

6. G.D. Roberts, D. C. Malarik, and J. O. Robaidek, "Viscoelastic Properties of Addition-Cured Polyimides Used in High Temperature Polymer Matrix Composites," Composites Design, Manufacturing, and Application; Proceedings of the Eighth International Conference on Composite Materials, S.W. Tsai and G.S. Springer, eds., Society for Advances of Materials and Process Engineering, Covina, CA, 1991, pp. 12–H–1 to 12–H–10.

7. S. Brunauer, The Adsorption of Gases and Vapor, Vol. 1, Princeton University Press, London, p. 120.

Specimen	Length (cm)	Width (cm)	Thickness (cm)	Surface Area^a (cm^2)			Edge (%)
				S_1	S_2	S_3	
T-3	8.94	10.83	0.13	193.64	2.32	2.82	2.6
T-5	8.94	10.83	0.28	193.64	5.00	6.06	5.4
T-9	9.27	1.56	0.13	28.92	2.41	0.41	8.7
T-12	8.94	10.83	0.70	193.64	12.52	15.16	12.5
T-27	8.90	10.20	1.75	181.56	31.15	35.70	27.0
T-50	4.51	1.80	1.30	16.24	12.45	4.68	50.3
T-73	6.35	0.71	1.75	9.02	22.22	2.48	73.0
T-89	10.10	0.21	1.75	9.02	4.24	0.74	89.0

Table 1. T650-35 graphite/PMR-15 composite dimensional data
^{a}See Figure 1

Specimen	Aging Time (hr)	Aging Temperature (°C)	Weight Loss (%)	Ethanol Permeability
T-3	1510	316	10.00	No permeation
T-9	1510	316	10.00	No permeation
T-73	1370	316	10.00	Trace of complete permeation
T-89	240	316	2.08	No permeation
T-89	500	316	6.82	Fully permeable
T-89	860	316	13.19	Fully permeable
T-89	2000	260	2.46	Isolated wet spots on back surface
T-89	2000	288	4.28	Permeable with some isolated dry spots

Table 2. Permeability of specimens to ethanol after air aging

Specimen	Weighing Condition	Mean, X (g)	Standard Deviation		95% Confidence Interval	
			(g)	(%)	(g)	(%)
T-9	Dry	2.5048	$\pm 2.28 \times 10^{-3}$	± 0.09	$\pm 5.16 \times 10^{-3}$	± 0.20
T-9	Wet	2.7211	$\pm 7.01 \times 10^{-3}$	± 0.26	$\pm 1.59 \times 10^{-3}$	± 0.59
T-9	Water	0.2192	$\pm 3.53 \times 10^{-3}$	± 1.61	$\pm 7.98 \times 10^{-3}$	± 3.64
T-73	Dry	12.8270	$\pm 3.55 \times 10^{-3}$	± 0.033	$\pm 8.03 \times 10^{-3}$	± 0.075
T-73	Wet	11.6661	$\pm 1.69 \times 10^{-2}$	± 0.14	$\pm 3.82 \times 10^{-2}$	± 0.33
T-73	Water	0.8392	$\pm 1.89 \times 10^{-2}$	± 2.25	$\pm 4.28 \times 10^{-2}$	± 5.09

Table 3. Statistical analysis of water retention in aged composites reinforced with T-650-35 carbon fabric [Repeat amount N is 10]

Specimen	Weight Pickup (g)				Weight Loss (%)
	Edge		Surface		
	Small	Long	Molded	All	
T-5	1.4876	2.1198	2.4354	2.4751	14.0
T-9	0.0027	0.0038	0.0021	0.0075	0.9
T-73	0.8404	0.8540	0.81043	1.1000	10.8

Table 4. Weight pickup as crack volume

Specimen	Water pickup (g/cm^2)				Weight loss (%)
	Edge		Surface		
	Small	Long	Molded	All	
T-5	0.6330	0.7440	0.012600	0.012500	14.0
T-9	.0068	.0016	.000073	.000524	0.9
T-73	.3419	.0390	.090000	.032000	10.8

Table 5. Water pickup as crack volume density

13
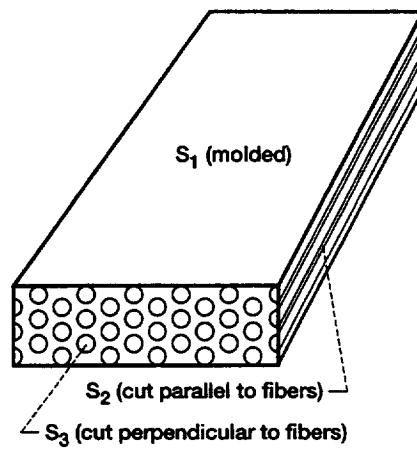
Figure 1.—Specimen surfaces.
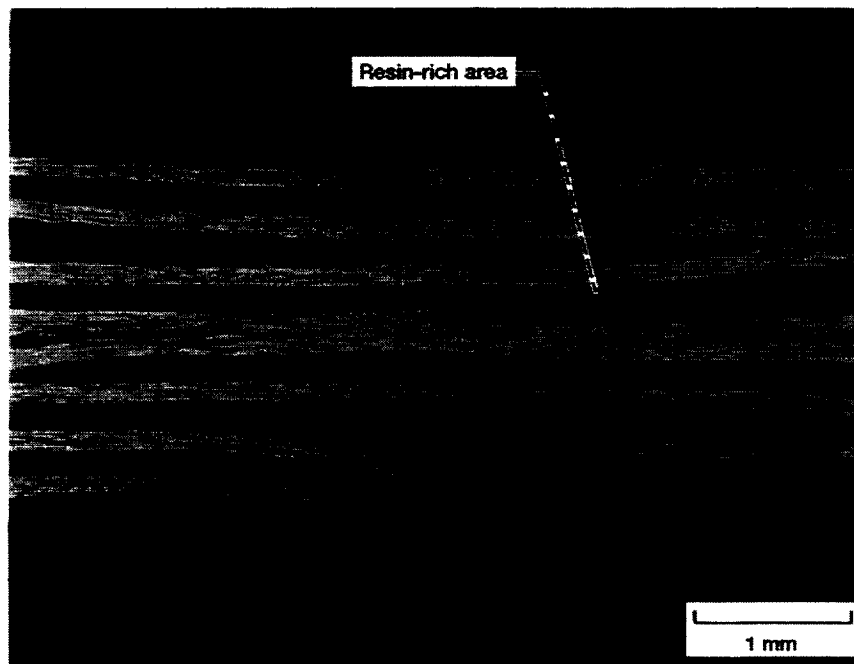
Figure 2.—T-650-35 8-harness fabric/PMR-15 composite unaged. Dark areas between tows are resin rich.

Exposed end
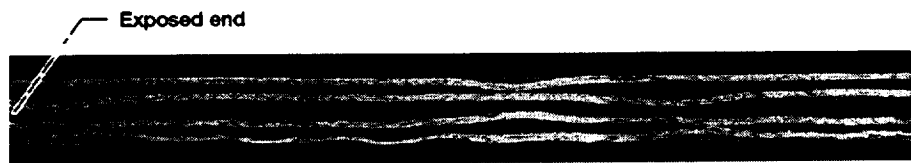
Figure 3.—T-3 specimen air aged for 500 hours at 316°C with 2% weight loss.

Exposed end
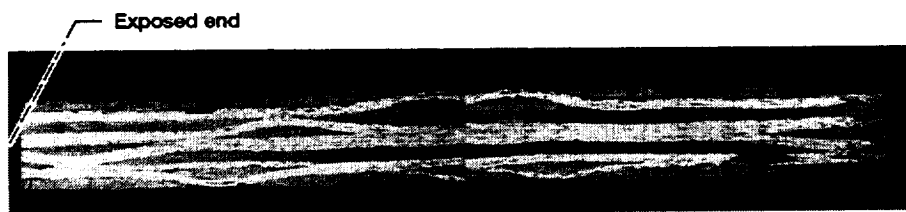
Figure 4.—T-3 specimen after air aging for 890 hours at 316°C with 4.4% weight loss.

Exposed end
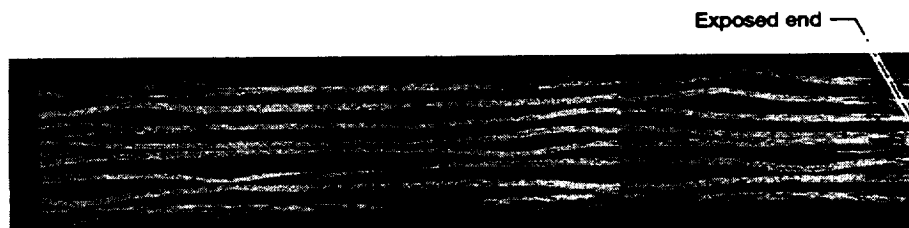
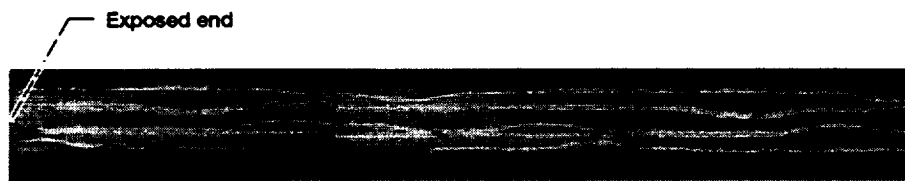Figure 5.—T-5 specimen air aged for 890 hours at 316°C with 2.9% weight loss.

15

Figure 6.—T-3 specimen air aged for 1510 hours at 316°C with 10% weight loss.
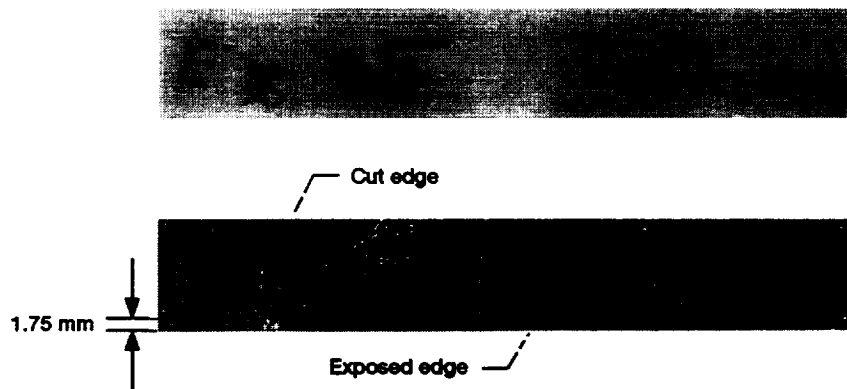
Figure 7.—T-3 panels air aged for 1510 hours at 316°C. Top image not enhanced with di-iodobutane.
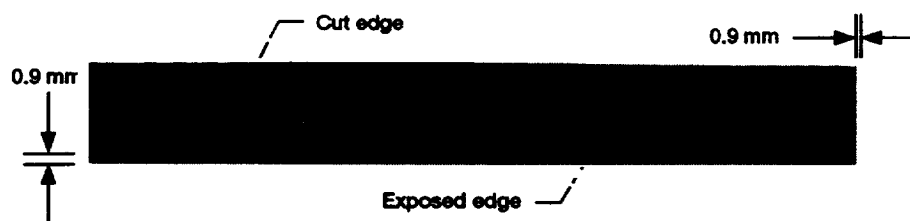
Figure 8.—T-5 panel air aged for 840 hours at 316°C with 2.9% weight loss.

16
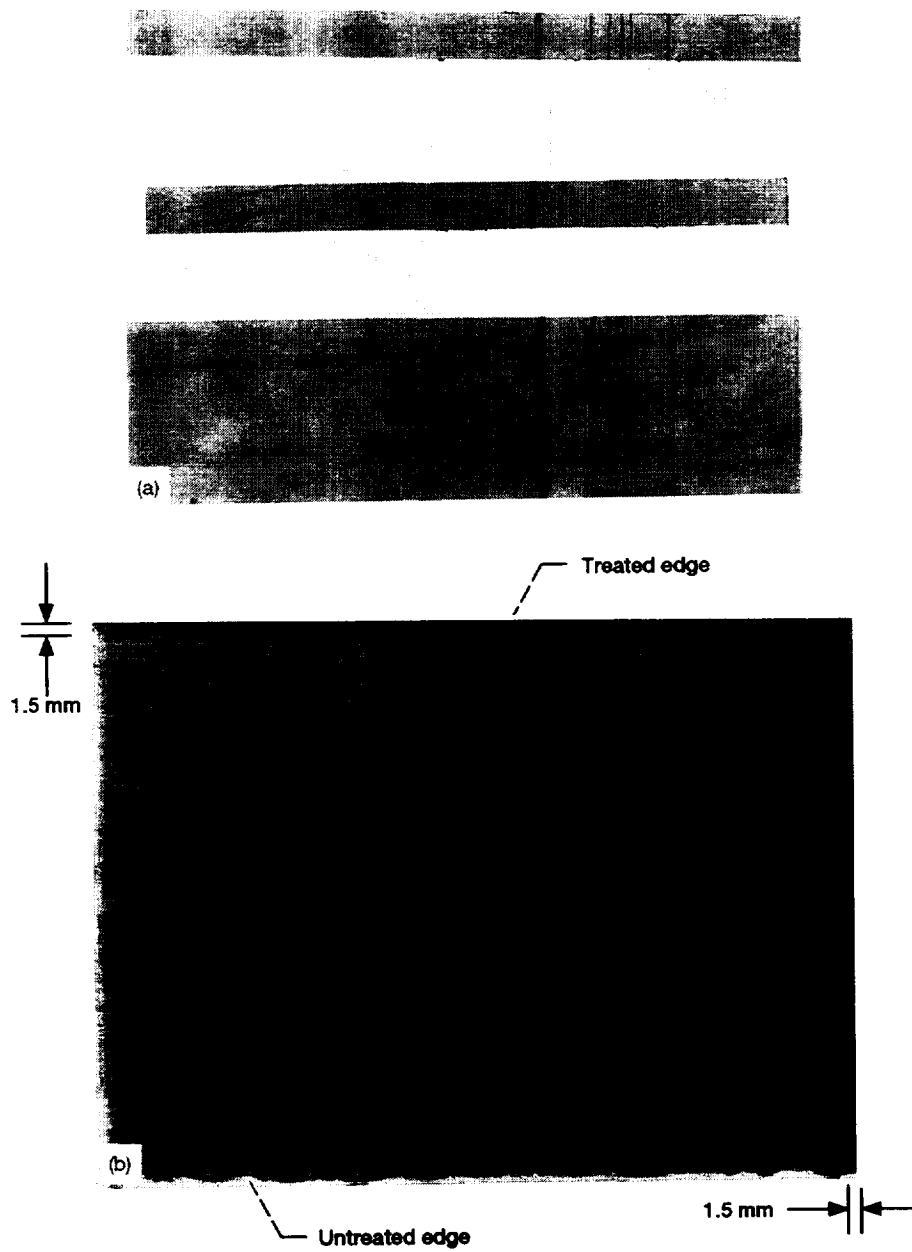
Figure 9.—T-5 laminate specimens treated with di-iodobutane. (a) Uaged. (b) Air aged for 1730 hours at 316°C with 9.6% weight loss.
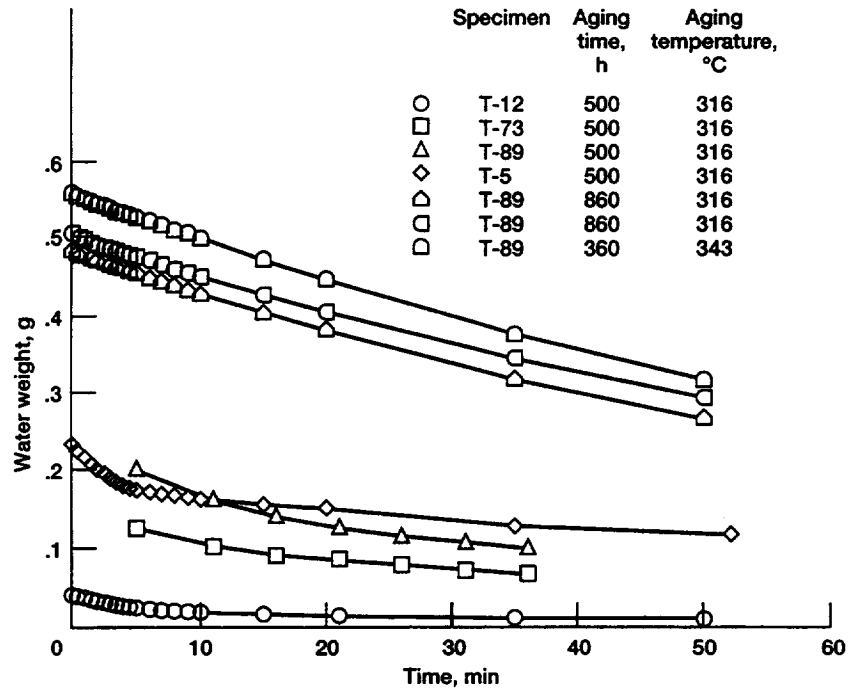
Figure 10.—Water immersion technique data from composites air aged at elevated temperatures. Numerical designations indicate nominal percent of surface area along edges.
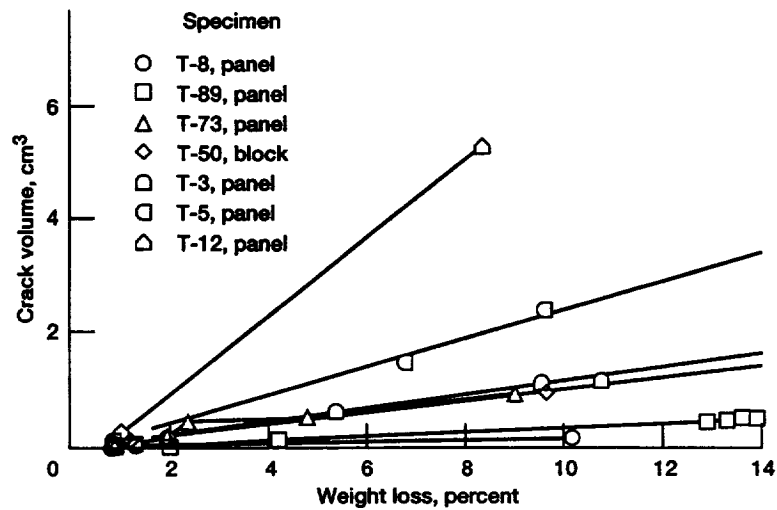
Figure 11.—Crack volumes of air-aged polymer matrix specimens reinforced with carbon fabric as function of percent weight loss. Numerical designations indicate nominal percent of surface area along edges.
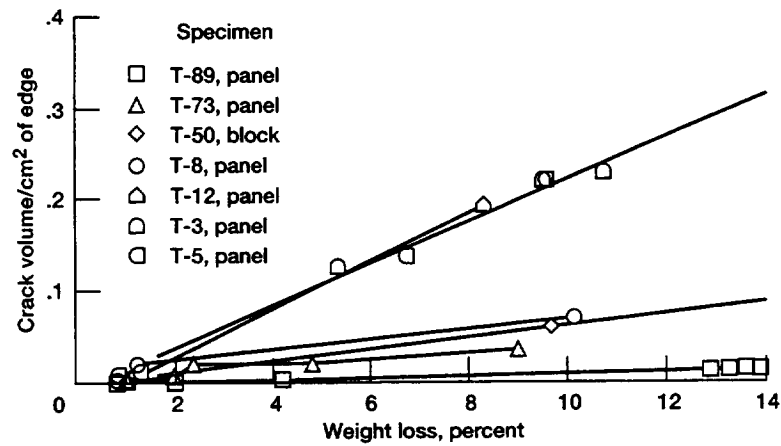
Figure 12.—Crack volumes per unit of edge area of air-aged composite plates as function of percent weight loss. Numerical designations indicate nominal percent of surface area along edges.
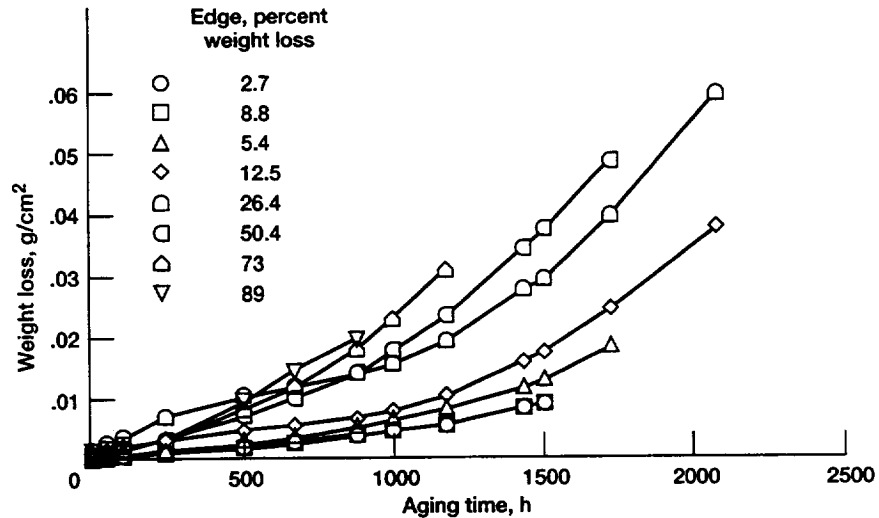
Figure 13.—Weight loss of air-aged fabric/PMR-15 composites at 316°C.

19
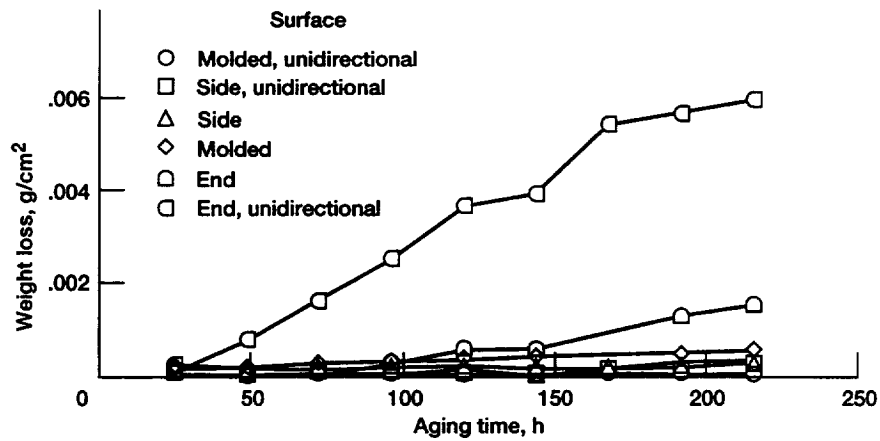
Figure 14.—Weight loss from specimen faces of carbon-fiber-reinforced composites air aged at 288°C.
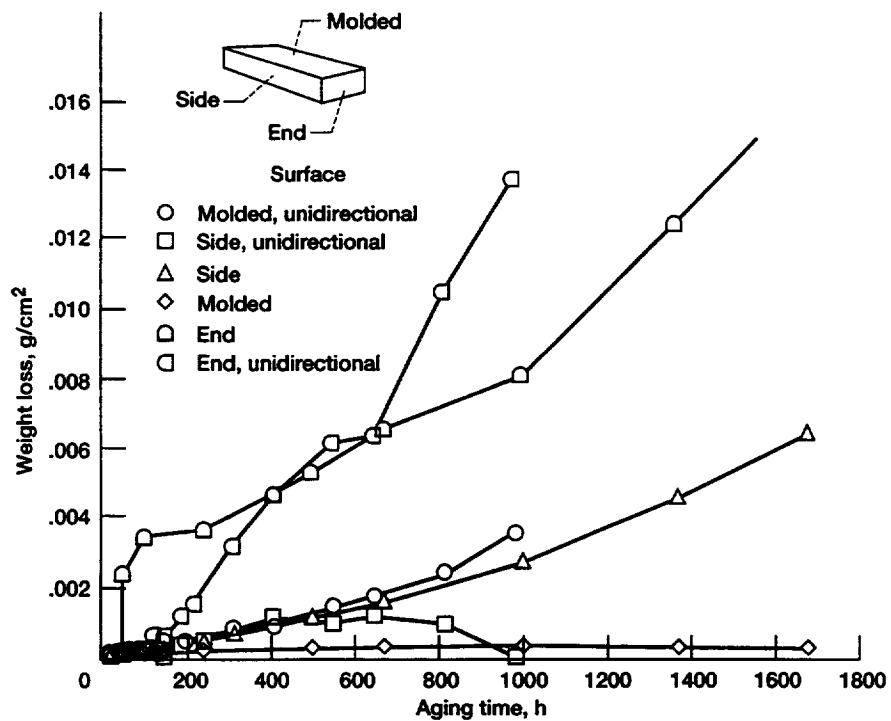

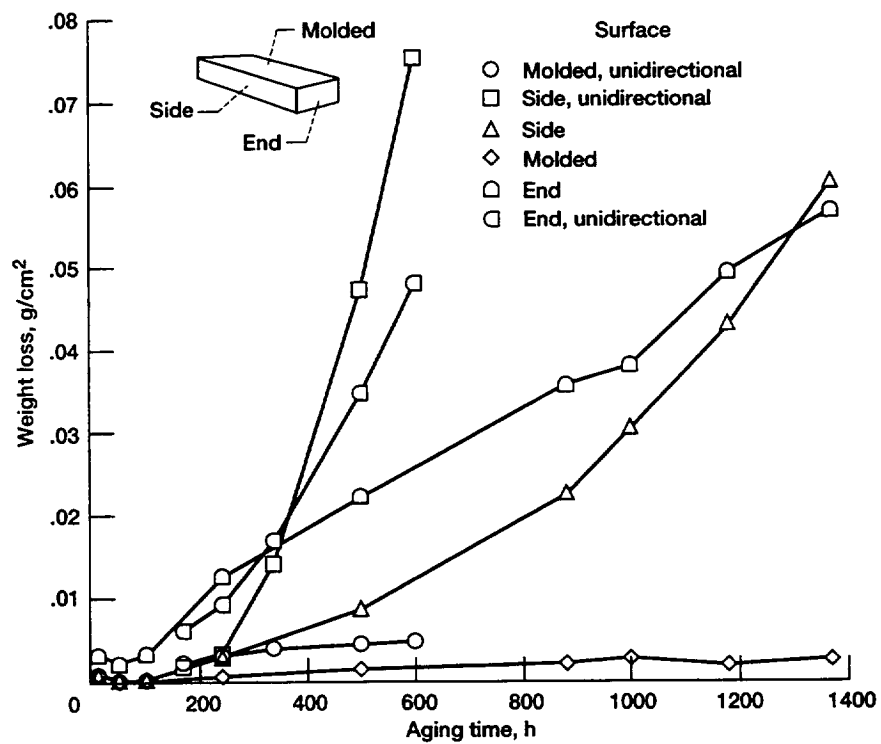Figure 15.—Weight loss from specimen faces of carbon-fiber-reinforced composite specimens air aged at 316°C.

Figure 16.—Weight loss from specimen faces of carbon-fiber-reinforced composite specimens air aged at 343°C.

REPORT DOCUMENTATION PAGE

Form Approved
OMB No. 0704-0188

1. AGENCY USE ONLY (Leave blank)	2. REPORT DATE	3. REPORT TYPE AND DATES COVERED
	July 1994	Technical Memorandum

4. TITLE AND SUBTITLE

Penetration of Carbon-Fabric-Reinforced Composites by Edge Cracks During Thermal Aging

5. FUNDING NUMBERS

WU–510–01–50

6. AUTHOR(S)

Kenneth J. Bowles and John E. Kamvouris

7. PERFORMING ORGANIZATION NAME(S) AND ADDRESS(ES)

National Aeronautics and Space Administration
Lewis Research Center
Cleveland, Ohio 44135–3191

8. PERFORMING ORGANIZATION REPORT NUMBER

E–8661

9. SPONSORING/MONITORING AGENCY NAME(S) AND ADDRESS(ES)

National Aeronautics and Space Administration
Washington, D.C. 20546–0001

10. SPONSORING/MONITORING AGENCY REPORT NUMBER

NASA TM–106530

11. SUPPLEMENTARY NOTES

Kenneth J. Bowles and John E. Kamvouris, NASA Lewis Research Center. Responsible person, Kenneth J. Bowles, organization code 5150, (216) 433–3197.

12a. DISTRIBUTION/AVAILABILITY STATEMENT

Unclassified - Unlimited
Subject Category 24

12b. DISTRIBUTION CODE

13. ABSTRACT (Maximum 200 words)

Thermo-oxidative stability (TOS) test results are significantly influenced by the formation and growth or presence of interlaminar and intralaminar cracks in the cut edges of all carbon-fiber-crosslinked, high temperature polymer matrix composites[1-5] (i.e., unidirectional, crossplied, angle-plied, and fabric composites). The thermo-oxidative degradation of these composites is heavily dependent on the surface area that is exposed to the harmful environment and on the surface-to-volume ratio of the structure under study. Since the growth of cracks and voids on the composite surfaces significantly increases the exposed surface areas, it is imperative that the interaction between the aging process and the formation of new surface area as the aging time progresses be understood.

14. SUBJECT TERMS

Composites; Cracks; Thermo-oxidative stability; Degradation

15. NUMBER OF PAGES
23

16. PRICE CODE
A03

17. SECURITY CLASSIFICATION OF REPORT	18. SECURITY CLASSIFICATION OF THIS PAGE	19. SECURITY CLASSIFICATION OF ABSTRACT	20. LIMITATION OF ABSTRACT
Unclassified	Unclassified	Unclassified	